Version of Record: https://www.sciencedirect.com/science/article/pii/S0981942821003302
Manuscript_745bfc0eead9a30d1160c4ee7915be1f

Invited mini-review

# Potassium dependency of enzymes in plant primary metabolism

Jing Cui[1] and Guillaume Tcherkez[1,2*]

1. Research School of Biology, ANU Joint College of Sciences, Australian National University, 2601 Canberra ACT, Australia.

2. Institut de Recherche en Horticulture et Semences, INRAe Angers, Université d'Angers, 42 rue Georges Morel, 49070 Beaucouzé, France.

*Contact author to whom correspondence should be addressed: guillaume.tcherkez@anu.edu.au; Tel. +61 2 6125 0381.

**Keywords:** potassium, enzymes, primary metabolism

**Number of figures:** 6

**Word count (w/o abstract and references):** 4,309

**Twitter account:** @IsoSeed

**ORCID accounts:**

G. Tcherkez: https://orcid.org/0000-0002-3339-956X

J. Cui: https://orcid.org/0000-0002-8096-9270



© 2021 published by Elsevier. This manuscript is made available under the CC BY NC user license
https://creativecommons.org/licenses/by-nc/4.0/

## Abstract

Potassium is a macroelement essential to many aspects of plant life, such as photosynthesis, phloem transport or cellular electrochemistry. Many enzymes in animals or microbes are known to be stimulated or activated by potassium ($K^+$ ions). Several plant enzymes are also strictly $K^+$-dependent, and this can be critical when plants are under K deficiency and thus intracellular $K^+$ concentration is low. Although metabolic effects of low K conditions have been documented, there is presently no review focusing on roles of $K^+$ for enzyme catalysis or activation in plants. In this mini-review, we compile the current knowledge on $K^+$-requirement of plant enzymes and take advantage of structural data to present biochemical roles of $K^+$. This information is instrumental to explain direct effects of low $K^+$ content on metabolism and this is illustrated with recent metabolomics data.

## Introduction

Potassium (K) is a major nutrient representing up to ≈5% of plant matter. K is essential for plant stomatal conductance and photosynthesis, phloem transport and cellular ion balance (Wang and Wu, 2013). In many cultivated areas where K availability is naturally low, K fertilisation is required, representing a global market of $12.6 billion per year (More, 2020). K fertilisation is of importance for high K-demanding crops such as oil palm, since some tropical soil types are relatively K-poor and waterlogging can limit further K assimilation (Cui et al., 2019b). In the past decade, intense efforts have been devoted to understanding molecular response mechanisms to K deficiency. Low K sensing involves CBL1/9 (calcineurin B like 1/9) and CIPK23 (CBL interacting protein kinase 23) via a $Ca^{2+}$ signal triggered by low K (Ródenas and Vert, 2020, Tagliani et al., 2020, Tang et al., 2020). CIPK23 in turn phosphorylates and activates the voltage-gated channel AKT1 (Lan et al., 2011, Sánchez-Barrena et al., 2020), and the transporter HAK5 (Ródenas et al., 2021) thereby enhancing $K^+$ absorption. Other targets of CIPK23 include KUP4 ($K^+$ uptake transporter) and the vacuolar channel TPK (two pores $K^+$) (reviewed in Ródenas and Vert, 2020).

Importantly, downstream events associated with low K conditions also include a reorchestration of metabolism, due to both indirect (regulatory mechanisms) and direct effects (use of $K^+$ as a cofactor) of $K^+$ scarcity. Indirect (regulatory) mechanisms seem to involve the central metabolic regulator mTOR, which interacts effectively with CIPK23 (Deng et al., 2020). Direct effects result from $K^+$ being involved in the activation of a myriad enzymes with a wide range of functions, a phenomenon that has been recognized for a long time (Suelter, 1970). Of course, not all of the enzymes exhibit strict $K^+$ dependency, since other monovalent cations such as $Na^+$, $Li^+$, $Rb^+$, $NH_4^+$ can replace $K^+$ (Gohara and Di Cera, 2016). However, as noticed early on by (Miller and Evans, 1957), the replacement of $K^+$ by other univalent cations on enzyme activation has generally been tested in vitro without considering natural ion concentrations in plant cells (where $K^+$ is the major cation) or their physiological relevance (in particular, $Rb^+$ and $Li^+$ are not naturally present at significant concentration).

$K^+$ activates enzymes by providing proper ionic strength (medium effect) or participating somehow to catalysis (e.g. forming a proper electrostatic environment in the active site for reactants, with a $K^+$-binding site) thus playing the role of a cofactor. In this case, $K^+$ coordination to the enzyme benefits to enzyme-substrate interactions and catalysis via either (*i*) $K^+$ direct contact with enzyme amino acid residues (like aspartate or glutamate) and/or the substrate within the active site, or (*ii*) binding to a separate site which in turn influences kinetic properties (Di Cera, 2006, Page and Di Cera, 2006, Gohara and Di Cera, 2016). In the past years, some progress has been made in the role of ions in the structure of enzymes, especially from Mammals and bacteria, shedding light on molecular mechanisms of binding and activation by $K^+$. For example, intense effort has been devoted to examining the well-known $K^+$-dependence of pyruvate kinase or arginase, the activity of which is considerably affected under K deficiency (see below). In this mini-review, we briefly describe $K^+$-dependent enzymes relevant for plant primary metabolism, mention the $K^+$ requirement for translational activity by the protein synthesis machinery and summarize the impact of $K^+$-dependence on metabolism when plants face low K availability, or K deficiency. Key $K^+$-dependent enzymes of primary C, N or S metabolism are replaced in their metabolic context in Fig. 1. In what follows, we shall focus on enzymes that bind $K^+$ and thus are affected by low $K^+$ concentration. $K^+$ binding sites of selected enzymes are compiled in Figs. 2 to 4.

## $K^+$-dependent enzymes in catabolism

### *Pyruvate kinase*

In the glycolytic pathway, pyruvate kinase (EC 2.7.1.40) catalyses the conversion of phospho*enol*pyruvate (PEP) and adenosine di-phosphate (ADP) to pyruvate and ATP. Pyruvate kinase from rat muscle is the first enzyme reported to be activated by $K^+$ (Boyer et al., 1942, Lardy and Ziegler, 1945). It was later demonstrated that the activity of this enzyme depends on univalent cations together with magnesium ($Mg^{2+}$) or manganese ($Mn^{2+}$) (Kachmar and Boyer, 1953, Mesecar and Nowak, 1997a, b). Pyruvate kinase from different plant species were also activated by $K^+$, with activation effect of $K^+$ saturating at about 50 mM (Miller and Evans, 1957, McCollum et al., 1958). The $K^+$-dependence of pyruvate kinase across lineages has been reviewed previously, and with the exception of some prokaryotic forms, all pyruvate kinase forms require a monovalent cation for catalysis (Muñoz and Ponce 2003). First structural studies of pyruvate kinase from yeast complexed with a substrate analogue phospho-glycolate and catalytic metal ions, manganese ($Mn^{2+}$) and $K^+$, has revealed that $K^+$ interacts closely with residues of the active site as well as substrates (Jurica et al., 1998). The structure of the enzyme with $K^+$ has also been resolved recently in *Plasmodium falciparum* (Fig. 2a) (Zhong et al., 2020). The active site of the enzyme is situated at the extremity of a β-barrel, and at least 5 oxygen atoms appear to be involved in the $K^+$ coordination sphere: -OH groups of two Ser and one Thr, -COOH group of Asp and critically, the γ-phosphate group of ATP (which is also coordinated to $Mg^{2+}$). This explains not only why $K^+$ is essential for the structure of the active site but also for stabilisation of the product (ATP). Interestingly, the structure of the $Na^+$-bound pyruvate kinase complex is similar to that with $K^+$ (Larsen et al.,, 1997), while the $k_{cat}$ of pyruvate kinase with $Na^+$ activation is about 8% only of that with $K^+$ (Kayne, 1971), suggesting $K^+$ either has function(s) other than the overall geometry of the active site, or that the active site is well suited for the ion radius of $K^+$ and not $Na^+$.

*Pyruvate dehydrogenase*

Pyruvate decarboxylase (subunit E1) together with dihydrolipoyl transacetylase (subunit E2) and dihydrolipoyl dehydrogenase (subunit E3) form the pyruvate dehydrogenase complex (PDC; EC 1.2.4.1). PDC catalyses the conversion of pyruvate to acetyl-CoA and $CO_2$ (coupled to the reduction of $NAD^+$ to NADH). It links glycolysis to the citric acid cycle. High potassium concentration (100 mM KCl) can increase pyruvate decarboxylation activity by 50–100% compared to low K (5 mM KCl) (Lai and Sheu, 1985). A stimulating role of $K^+$ in catalysis is supported by the fact that a pair of symmetrical $K^+$ binding sites, similar to branched chain ketoacid dehydrogenase (see below), have been found in the crystal structure of human and bacterial pyruvate dehydrogenase subunit E1 (Ciszak et al., 2003, Frank et al., 2004, Kato et al., 2008). $K^+$ plays a key role in structuring a loop between an α-helix and a β-sheet. The two $K^+$-binding sites are positioned perpendicularly to the substrate (thiamine binding sites) and are important for the overall conformation of the protein during catalysis.

*Succinyl-CoA thiokinase*

Succinyl-CoA thiokinase (EC 6.2.1.5 (ATP-dependent form) and EC 6.2.1.4 (GTP-dependent form); also known as succinyl coenzyme A synthetase, or succinate thiokinase) is an essential enzyme in tricarboxylic acid cycle catalysing the reversible conversion of succinyl-CoA to succinate. It requires $Mg^{2+}$ and is also activated by univalent cations, with $K^+$ being the most effective (Bush, 1969, Besford and Maw, 1976). $K^+$ appears necessary to facilitate magnesium binding and promote the reaction in the forward direction (succinyl-CoA cleavage to succinate, producing GTP in animals or ATP in plants) (Lynn and Guynn, 1978). Since $K^+$ binds succinate and succinyl-CoA very weakly, these old kinetics studies suggest that $K^+$ rather binds an enzyme amino acid residue and/or phosphate groups of the nucleotide. To date, only two structures with $K^+$ are available and are associated with the (GDP-dependent) pig enzyme (Fraser et al., 2006). $K^+$ binds to the enzyme at a site that is different from that

binding $Mg^{2+}$ and appears to coordinate phosphate groups of GTP as well as an aspartate residue of the protein (Asp 220). Therefore, $K^+$ seems to play an important role in stabilizing the formation the product (GTP) and thus to facilitate the equilibrium towards succinate + CoA-SH + GTP.

*Asparaginase*

The $K^+$-dependence of asparaginase is now very well documented. Asparaginase (EC 3.5.1.1) is an important enzyme for nitrogen metabolism since asparagine contains a high N-to-C ratio (one of the highest after arginine) and thus plays the role of a major nitrogen transport and storage compound in many higher plants, especially in carbon-limiting conditions or in Legumes (Lam et al., 1995, Lea et al., 2007). In leaf phloem exudates of *Arabidopsis*, from dark-grown or dark-adapted plants, asparagine is the major amino acid exported (Schultz, 1994). Asparagine is hydrolysed by asparaginase into aspartate and ammonia, and the latter can be subsequently reassimilated by glutamine synthetase thus forming glutamine. Therefore, it has been proposed that asparaginase play an important role in providing nitrogen to sink tissues including under N deficiency conditions, by processing asparagine into available ammonium (Curtis et al., 2018). Accordingly, asparaginase gene expression is mainly observed in developing tissues including apical meristems, expanding leaves, inflorescences and seeds (Grant and Bevan, 1994, Lea et al., 2007). Two classes of asparaginase exist in plants: $K^+$-dependent and $K^+$-independent. The presence $K^+$-dependent asparaginase was first shown in developing seeds of various plant species (Sodek et al., 1980). In the absence of $K^+$, asparaginase activity was hardly detectable in cotyledons and/or testa of *Pisum sativum*, *Pisum arvense*, *Phaseolus multiflorus*, *Lupinus albus*, *L. mutabilis* and *Zea mays* (Sodek et al., 1980). In these species, $K^+$ activation of asparaginase saturated at about 20 mM. $Na^+$ can activate asparaginase as well but it is much less effective, since 27 % only of enzyme activity can be achieved (relative to that with $K^+$) in the testa of *Pisum sativum* (Sodek et al., 1980). In *Arabidopsis*, recombinant $K^+$-dependent asparaginase (encoded by *At3g16150*) displays 80-fold higher catalytic efficiency with asparagine than that of the $K^+$-independent isoform (encoded by *At5g08100*), suggesting the former may metabolize asparagine more effectively in planta (Bruneau et al., 2006).

The mechanistic basis of $K^+$ activation in asparaginase catalysis has been studied in detail with the French bean (*Phaseolus vulgaris*) enzyme. Two studies using recombinant $K^+$-dependent asparaginase PvAspG1 from *Phaseolus vulgaris* showed that the addition of $K^+$ leads to an increase in the apparent $V_{max}$ and a decrease in the apparent $K_m$, although the two studies exhibit numerical differences in fold changes of $V_{max}$ and $K_m$ (Bejger et al., 2014, Ajewole et al., 2018). Overall, $K^+$ increases more than ten-fold the catalytic efficiency of PvAspG1 (Bejger et al., 2014, Ajewole et al., 2018). Crystal structures of PvAspG1 in the presence of $K^+$ or/and $Na^+$ revealed the mechanism of requirement of $K^+$ for activation of enzyme (Bejger et al., 2014). There are four metal binding sites in PvAspG1 with two in stabilization loops (residues Leu58–Arg68) and two in activation loops (residues Val111–Ser118). One of the loops is also present in $K^+$-independent asparaginases ("stabilization" loop), while the latter is not ("activation" loop). $K^+$ binding sites are outside the enzyme active site, suggesting the activation of $K^+$ is not via $K^+$ facilitating direct interaction of the active site with substrates. The binding of $Na^+$ or $K^+$ in the stabilization loop does not influence the enzyme active site, consistent with the fact they are present in both $K^+$-dependent and -independent asparaginases. The enzyme active site is located between the two loops.

$K^+$ binding in the activation loop (illustrated in Fig. 2b) changes the conformation, thereby allowing the binding or anchoring reaction substrate/products in the active site (by contrast, $Na^+$ binding does not allow such a motion). The importance and sufficiency of the activation loop for $K^+$ activation

of plant asparaginase is also supported by the effect of mutating Ser 118 to Ile in the $K^+$-dependent asparaginase (PvAspG1) or the corresponding residue (Ile-117) to Ser in the $K^+$-independent asparaginase (PvAspGT2) (Ajewole et al., 2018): in fact, changing Ile-117 in PvAspGT2 to Ser results in turning PvAspGT2 into a $K^+$-dependent asparaginase with catalytic efficiency increased 45-fold in the presence of $K^+$. Conversely, changing Ser to Ile in PvAspG1 abolishes $K^+$ activation.

*Branched-chain α-keto acid dehydrogenase*

The branched-chain α-keto acid dehydrogenase complex (BCKDC; EC 1.2.4.4) is involved in the catabolism of branched-chain amino acids (isoleucine, valine, and leucine). The activity and stability of BCKDC from rat liver strictly depends on $K^+$ (Shimomura et al., 1988). The presence of four $K^+$ binding sites has been shown in the crystal structure of human branched-chain α-keto acid dehydrogenase (BCKD) (Ævarsson et al., 2000); Wynn et al., 2004). BCKD is one of the subunits of BCKDC and resembles E1 of PDC. Two $K^+$ binding sites are perpendicular to thiamine binding sites and are very similar to that found in E1 of PDC. The two other $K^+$ binding sites are nearly in the same plane as thiamine binding sites at about 10 Å only. Here, $K^+$ maintains a loop (that comprises Thr 166 that coordinates $K^+$) that faces directly bound thiamine, and this allows good positioning of Leu 164 and Ser 162 side chains, which bend towards thiamine. Unsurprisingly, impeding $K^+$ binding by mutating the $K^+$ binding site (using a Thr 166-to-Met mutant) in human BCKD results in total loss of enzyme activity (Wynn et al., 2001).

**$K^+$-dependent enzymes in sugar metabolism**

*Fructose-1,6-bisphosphatase*

Fructose 1,6-bisphosphatase (EC 3.1.3.11) is a key enzyme in glycolysis and catalyses the hydrolysis of D-fructose 1,6-bisphosphate to D-fructose 6-phosphate and inorganic phosphate. $K^+$ functions as an activator of the enzyme. In fact, it has been shown that $K^+$ increases maximal velocity ($V_{max}$) of mammalian fructose 1,6-bisphosphatase (Hubert et al., 1970). Crystallographic structures of the enzyme from pig showed that three $K^+$ binding sites are present in each subunit, thus leading to a stoichiometry of twelve $K^+$ ions per homotetramer (Villeret et al., 1995). $K^+$ helps structuring the active site (which is close to the interface between subunits) since it binds Asp and Glu residues (Fig. 2c). Also, using a fructose 1,6-bisphosphate analogue (2,5-anhydro-1,6-di-O-phosphono-D-glucitol, APG), it was found that a phosphate group of APG directly participates in the coordination sphere of $K^+$. A similar structure has been found in the enzyme of *Leishmania* crystallised with $K^+$ and inorganic phosphate (Yuan et al., 2017). These results strongly suggest that $K^+$ facilitates the nucleophilic attack on the phosphorus centre and thus allows cleavage of the phospho-ester during catalysis.

*Starch synthase*

Th $K^+$-dependence of starch synthase (EC 2.4.1.21) is critical for plant metabolism. In fact, starch is one of the most important storage carbohydrate in plants, in particular in leaves, where the degradation of transitory starch provides carbon and energy to support sucrose export and plant growth at night (Graf and Smith, 2011). Also, in starchy seeds, it provides carbon and energy for germination and seedling establishment (Zeeman et al., 2010). Starch synthase catalyses the biosynthesis of starch by adding glucose from ADP-glucose to the pre-existing glucose chains via α-1,4-linkage (glycosyl-transferring activity). $K^+$ stimulates the activity of starch synthase from a wide range of plants including maize, Legumes (bush beans, peas, soybeans), wheat, and potatoes (Nitsos and Evans, 1969). The optimum $K^+$ concentration for starch synthase activity is equivalent to concentrations normally found

in plant cells, about 75-100 mM (Nitsos and Evans, 1969). $Na^+$ and $Li^+$ can also activate starch synthase but are less effective than $K^+$. Surprisingly, the mechanism of potassium activation is still rather unclear. Crystal structures of starch synthase from *Arabidopsis*, the glaucophyte *Cyanophora paradoxa* and barley (*Hordeum vulgare*) have been resolved (Cuesta-Seijo et al., 2013, Nielsen et al., 2018), but these proteins were crystallized in the absence of $K^+$, thereby no structural direct information about the role of $K^+$ can be obtained for these structures. A very similar enzyme, glycogen synthase from *Pyrococcus abyssi*, has been crystallised with $K^+$ (Diaz et al., 2011). Three $K^+$ ions have been found, among which two are at the protein surface, and one coordinated to a Glu residue (Glu 339). When superposed to the structure of glycogen synthase from *E. coli* crystallised with glucose (Sheng et al., 2009), it appears clearly that $K^+$ binds within the active site at a very close distance of glucose, and thus is probably involved (along with $Mg^{2+}$ or $Mn^{2+}$) in the coordination of phosphate groups of the ADP moiety of ADP-glucose, thus facilitating catalysis (Fig. 3).

*β-amylase*

Starch degradation plays important roles in plant growth and development and in the stress response (Lloyd et al., 2005, Sulpice et al., 2009, Zeeman et al., 2010, Streb and Zeeman, 2012). A series of enzymes mediates the degradation of starch, among which β-amylase (BAM; EC 3.2.1.2) is crucial (Stitt and Zeeman, 2012). BAM is an exohydrolase, hydrolyzing the α-1,4 glucosidic linkage of starch from non-reducing ends to liberate successive β-maltose units. BAM2 is one of the nine BAMs in *Arabidopsis* (Monroe and Storm, 2018). BAM2 was initially shown to have negligible activity without $K^+$ (Fulton et al., 2008, Li et al., 2009), and Monroe et al., (2017) demonstrated that BAM2 requires $K^+$ for activity with maximal activity, at 80 mM and above. That is, the use of β-amylase assays without addition of salts in previous reports probably explains the observed low activity of BAM2. Other univalent cations such as $Li^+$, $Na^+$, $Rb^+$ and $Cs^+$ have a similar effect as $K^+$. In addition, monovalent ions are not present in any crystallized plant BAMs (where the active site residues are well-conserved across species). These led Monroe et al., (2017) to propose that the role of $K^+$ may be limited to providing sufficient ionic strength for BAM2 activity. Still, it is possible that $K^+$ forms part of the enzyme structure: $K^+$ may not bind to the active site, like other $K^+$-activated enzymes that are stimulated by $K^+$-binding outside the active site (Gohara and Di Cera, 2016). This is typically the case for asparaginase (discussed above), where $K^+$ binding to the activation loop affects the overall conformation of enzyme thereby affecting catalytic activity (Bejger et al.,, 2014). Also, the absence of ion(s) in published BAMs crystal structures may not be representative of the situation in BAM2, which requires $K^+$ for maximal activity. Future studies of the crystal structure of BAM2 in the presence of univalent cations will shed light on whether $K^+$ forms part of the structure of BAM2 or simply provide ionic strength.

**$K^+$ dependency in methylation: S-adenosylmethionine synthase**

S-adenosylmethionine (SAM) is the major methyl donor in myriads biochemical reactions, such as DNA methylation, or phospholipid synthesis. In addition, SAM functions in the aminopropylation pathway and transulfuration pathway (S assimilation) which are involved in the synthesis of polyamines and glutathione, respectively. This pathway is in turn of importance under $K^+$ deficiency since low K availability leads to polyamine accumulation and affects sulphur metabolism (Cui et al., 2020; Cui et al., 2021). The formation of SAM from methionine and ATP is catalysed by SAM synthase (EC 2.5.1.6; also referred to as methionine adenosyltransferase), which absolutely requires $K^+$ (Mudd and Cantoni, 1958). The study of the crystal structure of *E. coli* SAM synthase in the presence of an ATP analogue and methionine, $Mg^{2+}$ and $K^+$ has shown that $K^+$ is present in the active site and plays a key role in maintaining the active site geometry (Komoto et al., 2004). In fact, $K^+$ is coordinated to two acidic

residues (Asp 238 and Glu 42) as well as phosphate groups of pyrophosphate (often abbreviated as PPi) coming from ATP, as suggested by the proximity to the PPi analogue (diphosphono)aminophosphonic acid (Fig. 4a). The structure of the plant enzyme has been resolved recently in *Medicago truncatula* (Sekula et al., 2020). Homologous acidic residues are present (Asp 249, Glu 46) and the position of the potential substrate binding pocket might accommodate a coordination bond of the -COOH group of SAM with $K^+$ or, like in the bacterial enzyme, PPi coordination to $K^+$ (Fig. 4b). Although the specific role of $K^+$ during catalysis remains to be established, its strategic position at the centre of the active site and coordination to PPi suggests that it facilitate ATP cleavage and thus the formation of the C-S bond to form SAM.

**$K^+$ requirement for protein synthesis**

$K^+$ is required for protein synthesis (Blaha et al., 2000). In plants, $K^+$ has been shown to be required both in vitro (ribosome-mediated GTP hydrolysis), and in vivo ($^{15}N$-incorporation into proteins) protein synthesis (Amberger, 1975). As such, when plants are under K-deficient condition, protein synthesis is disturbed despite high nitrogen (N) availability. As a result, protein precursors such as amino acids, amides and nitrate accumulate (Armengaud et al., 2009, Wang et al., 2012), and $K^+$ deficiency tends to inhibit nitrogen assimilation. Similarly, in *E. coli*, it has been first suggested that decreased cell $K^+$ limits the rate of cell growth by a specific effect on protein synthesis (Lubin and Ennis, 1964). In fact, $K^+$ is primarily required for ribosome structure: hundreds of potassium ions have been shown to be present in *Thermus thermophilus* 70S ribosomes structure and many were in crucial positions within the ribosome such as codon-decoding and peptidyl transferase domains (Rozov et al.,, 2019). $K^+$ ions associated with ribosomes are believed to be essential to stabilize mRNA binding so as to maintain the correct frame position during elongation, stabilize tRNA ligands, and reinforce rRNA–protein interactions (Rozov et al., 2019).

**Direct consequences for metabolism**

The effect of low $K^+$ availability on metabolism has been examined for a long time, with the discovery of typical metabolites accumulated under K deficiency, like putrescine (which was found decades ago). However, the analysis of the broad picture is relatively recent, with detailed metabolomics analyses in Arabidopsis (Armengaud et al., 2009), sunflower (Cui et al., 2019a) and oil palm (Cui et al., 2019b). To date, oil palm is certainly the best characterized species for the description of metabolomics under K deficiency, including the interaction with plant age (Cui et al., 2019b). A summary of metabolomics results is provided in Fig. 5 and metabolic pathways are shown in Fig. 6. As mentioned above in the *Introduction*, some of the effects of low K conditions on metabolism are due to the direct effect of decreased $K^+$ concentration in the cytosol, which has effectively been shown to be lower (Armengaud et al., 2009). These direct effects will be discussed here since they illustrate the $K^+$-dependency of enzymes described above.

The most important effect seems to be on pyruvate kinase activity, leading to a restriction of the flux through glycolysis. This leads to the induction of alternative pathways: PEP carboxylation to oxaloacetate, reduction to malate and malate decarboxylation to pyruvate (in *Arabidopsis*), or parapyruvate shunt (in oil palm). In addition, the restriction on succinate thiokinase leads to an increase in citrate metabolism, with the accumulation of itaconate and/or citramalate produced from aconitate. As a result, several organic acids of the Krebs cycle tend to accumulate, and they appear in the cluster of metabolites generally more abundant under low K (group B, Fig. 5a). It is possible that aconitase itself is impacted by low $K^+$ conditions via oxidative stress and possible production of NO and $H_2O_2$

which are both aconitase inhibitors (in practice, they inhibit the second step of the reaction, preventing aconitate from being converted to isocitrate, thereby causing aconitate build-up). An important direct effect of low K conditions also concerns sugar metabolism. First, starch degradation is slowed down due to β-amylase $K^+$-dependency and thus starch content in leaves tends to be higher. In oil palm, the increased starch content is the most visible symptom of K deficiency in leaflet sugars (major soluble sugars are not significantly affected) (Fig. 5b). Conversely, there is a very clear impact on soluble sugars in oil palm rachis, suggesting a decrease in phloem movement velocity (Fig. 5b). This is a consequence of the well-known dependence of active transport driven by both $H^+$ and $K^+$ across phloem cell membranes (Dreyer et al., 2017). This restriction leads to the induction of raffinose and galactose metabolism in leaflet, which represents an alternative pathway to export sugars (group B, Fig. 5a; and top reactions, Fig. 6). Finally, the well-known low K biomarker, putrescine, is accumulated due to the induction of arginine decarboxylase (*Arabidopsis*) and/or ornithine decarboxylase (other species). The accumulation is also maybe caused by the inhibition of SAM synthase (discussed above), since SAM is required to convert putrescine into other polyamines (spermidine, spermine).

## Conclusions and perspectives

Taken as a whole, several enzymes that are crucial for primary carbon and nitrogen metabolism depend on $K^+$. The requirement for $K^+$ of enzyme catalysis participates in explaining the multiple effects of $K^+$ deficiency. However, several aspects are still awaiting further clarification, such as specific mechanisms of $K^+$ activation in enzymes where available crystal structure do not comprise $K^+$ ions (like BAM2 in *Arabidopsis*). Also, uncertainty remains as to whether enzymes that do not depend on $K^+$ for catalysis nevertheless require $K^+$ in the reactional medium to provide the proper electrostatic environment (ion strength effect). Also, potential isotope fractionation in $K^+$ binding is not documented yet. In fact, potassium is present in the form of three natural stable isotopes, $^{39}K$ (93.26%), $^{40}K$ (0.01%) and $^{41}K$ (6.73%). It is well-known that $K^+$ coordination and crystallisation in minerals fractionate between K isotopes, with changes in $\delta^{41}K$ ($^{41}K$ natural abundance) of about 1‰ between minerals and seawater and furthermore, weathering of silicates fractionates between K isotopes (Li et al., 2019). In plants, in has been recently shown that tissues are $^{41}K$-depleted compared to the nutrient solution, suggesting a fractionation of about 0.8‰ during K uptake by roots (Christensen et al., 2018). It is also likely that $K^+$ coordination in enzyme active sites also fractionates between isotopes since it involves desolvation and formation of $K^+$---$O^-$ bonds (typically with Glu or Asp residues). The knowledge of $^{39}K/^{41}K$ isotope effect in $K^+$ binding by enzymes would not only help to understand the isotope composition in plants, but also provide insights on the chemical mechanism of $K^+$ strong binding by active sites.

## Acknowledgements

The authors acknowledge the financial support of the Région Pays de la Loire and Angers Loire Métropole via the grant Connect Talent Isoseed awarded to G.T.

## Data availability

There is no data associated with this manuscript.

## References


Ævarsson A., Chuang J.L., Max Wynn R., Turley S., Chuang D.T., Hol W.G.J., 2000. Crystal structure of human branched-chain α-ketoacid dehydrogenase and the molecular basis of multienzyme complex deficiency in maple syrup urine disease. Structure 8 (3), 277-291.

Ajewole E., Santamaria-Kisiel L., Pajak A., Jaskolski M., Marsolais F., 2018. Structural basis of potassium activation in plant asparaginases. The FEBS Journal 285 (8), 1528-1539.

Amberger, A., 1975. Protein biosynthesis and effect of plant nutrients on the process of protein formation. In Proceedings of the 11th Colloquium of the Int. Potash Institute, pp. 75-89.

Armengaud P., Sulpice R., Miller A.J., Stitt M., Amtmann A., Gibon Y., 2009. Multilevel analysis of primary metabolism provides new insights into the role of potassium nutrition for glycolysis and nitrogen assimilation in *Arabidopsis* roots. Plant Physiol. 150 (2), 772-785.

Bejger M., Imiolczyk B., Clavel D., Gilski M., Pajak A., Marsolais F., Jaskolski M., 2014. $Na^+/K^+$ exchange switches the catalytic apparatus of potassium-dependent plant L-asparaginase. Acta Crystallographica Section D 70 (7), 1854-1872.

Besford R.T., Maw G.A., 1976. Effect of potassium nutrition on some enzymes of the tomato plant. Annals Bot. 40 (3), 461-471.

Blaha G., Stelzl U., Spahn C.M., Agrawal R.K., Frank J., Nierhaus K.H., 2000. Preparation of functional ribosomal complexes and effect of buffer conditions on tRNA positions observed by cryoelectron microscopy. Methods Enzymol. 317, 292-309.

Boyer P.D., Lardy H.A., Phillips P.H., 1942. The role of potassium in muscle phosphorylations. J. Biol. Chem. 146 (2), 673-682.

Bruneau L., Chapman R., Marsolais F., 2006. Co-occurrence of both L-asparaginase subtypes in *Arabidopsis* At3g16150 encodes a $K^+$-dependent L-asparaginase. Planta 224 (3), 668-679.

Bush L.P., 1969. Influence of certain cations on activity of succinyl-CoA synthetase from tobacco. Plant Physiol. 44 (3), 347-350.

Christensen, J. N., Qin, L., Brown, S. T., DePaolo, D. J., 2018. Potassium and calcium isotopic fractionation by plants (soybean *Glycine max*, rice *Oryza sativa*, and wheat *Triticum aestivum*). ACS Earth and Space Chem. 2 (7), 745-752.

Ciszak E.M., Korotchkina L.G., Dominiak P.M., Sidhu S., Patel M.S., 2003. Structural basis for flip-flop action of thiamin pyrophosphate-dependent enzymes revealed by human pyruvate dehydrogenase. J. Biol. Chem. 278 (23), 21240-21246.

Cuesta-Seijo J.A., Nielsen M.M., Marri L., Tanaka H., Beeren S.R., Palcic M.M., 2013. Structure of starch synthase I from barley: insight into regulatory mechanisms of starch synthase activity. Acta Crystallographica Section D 69 (6), 1013-1025.

Cui, J., Abadie, C., Carroll, A., Lamade, E., Tcherkez, G., 2019a. Responses to K deficiency and waterlogging interact via respiratory and nitrogen metabolism. Plant Cell Environ. 42 (2), 647-658.

Cui J., Davanture M., Zivy M., Lamade E., Tcherkez G., 2019b. Metabolic responses to potassium availability and waterlogging reshape respiration and carbon use efficiency in oil palm. New Phytol. 223 (1), 310-322.

Cui, J., Lamade, E., Tcherkez, G., 2020. Potassium deficiency reconfigures sugar export and induces catecholamine accumulation in oil palm leaves. Plant Sci. 300, 110628.

Cui, J., Davanture, M., Lamade, E., Zivy, M., Tcherkez, G., 2021. Plant low-K responses are partly due to Ca prevalence and the low-K biomarker putrescine does not protect from Ca side effects but acts as a metabolic regulator. Plant Cell Environ. 44 (5), 1565-1579.

Curtis T.Y., Bo V., Tucker A., Halford N.G., 2018. Construction of a network describing asparagine metabolism in plants and its application to the identification of genes affecting asparagine metabolism in wheat under drought and nutritional stress. Food Energy Secur. 7 (1), e00126-e00126.

Deng K., Wang W., Feng L., Yin H., Xiong F., Ren M., 2020. Target of rapamycin regulates potassium uptake in *Arabidopsis* and potato. Plant Physiol. Biochem. 155, 357-366.

Díaz, A., Martínez-Pons, C., Fita, I., Ferrer, J. C., Guinovart, J. J., 2011. Processivity and subcellular localization of glycogen synthase depend on a non-catalytic high affinity glycogen-binding site. J. Biol. Chem. 286(21), 18505-18514.

Di Cera E., 2006. A structural perspective on enzymes activated by monovalent cations. J. Biol. Chem. 281 (3), 1305-1308.

Dreyer, I., Gomez-Porras, J. L., Riedelsberger, J., 2017. The potassium battery: a mobile energy source for transport processes in plant vascular tissues. New Phytol. 216 (4), 1049-1053.

Fulton D.C., Stettler M., Mettler T., Vaughan C.K., Li J., Francisco P., Gil M., Reinhold H., Eicke S., Messerli G., Dorken G., Halliday K., Smith A.M., Smith S.M., Zeeman S.C., 2008. β-AMYLASE4, a noncatalytic protein required for starch breakdown, acts upstream of three active β-amylases in *Arabidopsis* chloroplasts. The Plant Cell 20 (4), 1040-1058.

Gohara D.W., Di Cera E., 2016. Molecular mechanisms of enzyme activation by monovalent cations. J. Biol. Chem. 291 (40), 20840-20848.

Graf A., Smith A.M., 2011. Starch and the clock: the dark side of plant productivity. Trends Plant Sci. 16 (3), 169-175.

Grant M., Bevan M.W., 1994. Asparaginase gene expression is regulated in a complex spatial and temporal pattern in nitrogen-sink tissues. Plant J. 5 (5), 695-704.

Hubert E., Villanueva J., Gonzalez A.M., Marcus F., 1970. Univalent cation activation of fructose 1,6-diphosphatase. Archives Biochem. Biophys. 138 (2), 590-597.

Jurica M.S., Mesecar A., Heath P.J., Shi W., Nowak T., Stoddard B.L., 1998. The allosteric regulation of pyruvate kinase by fructose-1,6-bisphosphate. Structure 6 (2), 195-210.

Kachmar J.F., Boyer P.D., 1953. Kinetic analysis of enzyme reactions: II. the potassium activation and calcium inhibition of pyruvic phosphoferase. J. Biol. Chem. 200 (2), 669-682.

Komoto J., Yamada T., Takata Y., Markham G.D., Takusagawa F., 2004. Crystal Structure of the S-adenosylmethionine synthetase ternary complex: a novel catalytic mechanism of S-adenosylmethionine synthesis from ATP and Met. Biochemistry 43 (7), 1821-1831.

Lai J.C.K., Sheu K.-F.R., 1985. Relationship between activation state of pyruvate dehydrogenase complex and rate of pyruvate oxidation in isolated cerebro-cortical mitochondria: effects of potassium ions and adenine nucleotides. J. Neurochem. 45 (6), 1861-1868.

Lam H.M., Coschigano K., Schultz C., Melo-Oliveira R., Tjaden G., Oliveira I., Ngai N., Hsieh M.H., Coruzzi G., 1995. Use of *Arabidopsis* mutants and genes to study amide amino acid biosynthesis. The Plant Cell 7 (7), 887-898.

Lan W.-Z., Lee S.-C., Che Y.-F., Jiang Y.-Q., Luan S., 2011. Mechanistic analysis of AKT1 regulation by the CBL–CIPK–PP2CA interactions. Molecular Plant 4 (3), 527-536.

Lardy H.A., Ziegler J.A., 1945. The enzymatic synthesis of phosphopyruvate from pyruvate. J. Biol. Chem. 159 (2), 343-351.

Lea P.J., Sodek L., Parry M.A.J., Shewry P.R., Halford N.G., 2007. Asparagine in plants. Annals Appl. Biol. 150 (1), 1-26.

Li J., Francisco P., Zhou W., Edner C., Steup M., Ritte G., Bond C.S., Smith S.M., 2009. Catalytically-inactive β-amylase BAM4 required for starch breakdown in *Arabidopsis* leaves is a starch-binding-protein. Archives Biochem. Biophys. 489 (1), 92-98.

Li, S., Li, W., Beard, B. L., Raymo, M. E., Wang, X., Chen, Y., Chen, J., 2019. K isotopes as a tracer for continental weathering and geological K cycling. Proc. Natl. Acad. Sci. 116 (18), 8740-8745.

Lloyd J.R., Kossmann J., Ritte G., 2005. Leaf starch degradation comes out of the shadows. Trends Plant Sci. 10 (3), 130-137.

Lubin M., Ennis H.L., 1964. On the role of intracellular potassium in protein synthesis. Biochimica Biophysica Acta 80, 614-631.

McCollum R.E., Hageman R.H., Tyner E.H., 1958. Influence of potassium on pyruvic kinase from plant tissue. Soil Sci. 86 (6), 324-331.

Mesecar A.D., Nowak T., 1997a. Metal-ion-mediated allosteric triggering of yeast pyruvate kinase 2. A multidimensional thermodynamic linked-function analysis. Biochemistry 36 (22), 6803-6813.

Mesecar A.D., Nowak T., 1997b. Metal-ion-mediated allosteric triggering of yeast pyruvate kinase. 1. A multidimensional kinetic linked-function analysis. Biochemistry 36 (22), 6792-6802.

Miller G., Evans H.J., 1957. The influence of salts on pyruvate kinase from tissues of higher plants. Plant Physiol. 32 (4), 346-354.

Monroe J.D., Storm A.R., 2018. Review: The *Arabidopsis* β-amylase (BAM) gene family: Diversity of form and function. Plant Sci. 276, 163-170.

More A. (2020) Global potassium chloride market size. Research Reports 360, 13841629.

Mudd S.H., Cantoni G.L., 1958. Activation of methionine for transmethylation: III. The methionine-activating enzyme of bakers' yeast. J. Biol. Chem. 231 (1), 481-492.

Nielsen M.M., Ruzanski C., Krucewicz K., Striebeck A., Cenci U., Ball S.G., Palcic M.M., Cuesta-Seijo J.A., 2018. Crystal structures of the catalytic domain of *Arabidopsis thaliana* starch synthase IV, of granule bound starch synthase from CLg1 and of granule bound starch synthase I of *Cyanophora paradoxa* illustrate substrate recognition in starch synthases. Frontiers Plant Sci. 9 (1138)

Nitsos R.E., Evans H.J., 1969. Effects of univalent cations on the activity of particulate starch synthetase. Plant Physiol. 44 (9), 1260-1266.

Page M.J., Di Cera E., 2006. Role of $Na^+$ and $K^+$ in enzyme function. Physiol. Rev. 86 (4), 1049-1092.

Ródenas R., Vert G., 2020. Regulation of root nutrient transporters by CIPK23: 'one kinase to rule them all'. Plant Cell Physiol., Article no. pcaa156.

Ródenas R., Ragel P., Nieves-Cordones M., Martínez-Martínez A., Amo J., Lara A., Martínez V., Quintero F.J., Pardo J.M., Rubio F., 2021. Insights into the mechanisms of transport and regulation of the *Arabidopsis* high-affinity $K^+$ transporter HAK5. Plant Physiol., In press.

Rozov A., Khusainov I., El Omari K., Duman R., Mykhaylyk V., Yusupov M., Westhof E., Wagner A., Yusupova G., 2019. Importance of potassium ions for ribosome structure and function revealed by long-wavelength X-ray diffraction. Nature Commun. 10 (1), 2519.

Sánchez-Barrena M.J., Chaves-Sanjuan A., Raddatz N., Mendoza I., Cortés Á., Gago F., González-Rubio J.M., Benavente J.L., Quintero F.J., Pardo J.M., Albert A., 2020. Recognition and activation of the plant AKT1 potassium channel by the kinase CIPK23. Plant Physiol. 182 (4), 2143-2153.

Sekula, B., Ruszkowski, M., Dauter, Z., 2020. S-adenosylmethionine synthases in plants: Structural characterization of type I and II isoenzymes from *Arabidopsis thaliana* and *Medicago truncatula*. Intl. J. Biol. Macromol. 151, 554-565.

Sheng, F., Jia, X., Yep, A., Preiss, J., Geiger, J. H., 2009. The crystal structures of the open and catalytically competent closed conformation of *Escherichia coli* glycogen synthase. J. Biol. Chem. 284(26), 17796-17807.

Shimomura Y., Kuntz M.J., Suzuki M., Ozawa T., Harris R.A., 1988. Monovalent cations and inorganic phosphate alter branched-chain α-ketoacid dehydrogenase-kinase activity and inhibitor sensitivity. Archives Biochem. Biophys. 266 (1), 210-218.

Sodek L., Lea P.J., Miflin B.J., 1980. Distribution and properties of a potassium-dependent asparaginase isolated from developing seeds of *Pisum sativum* and other plants. Plant Physiol. 65 (1), 22-26.

Stitt M., Zeeman S.C., 2012. Starch turnover: pathways, regulation and role in growth. Curr. Op. Plant Biol. 15 (3), 282-292.

Streb S., Zeeman S.C., 2012. Starch metabolism in *Arabidopsis*. The Arabidopsis book 10, Chapter no. e0160.

Suelter C.H., 1970. Enzymes activated by monovalent cations. Science 168 (3933), 789-795.

Sulpice R., Pyl E.T., Ishihara H., Trenkamp S., Steinfath M., Witucka-Wall H., Gibon Y., Usadel B., Poree F., Piques M.C., Von Korff M., Steinhauser M.C., Keurentjes J.J., Guenther M., Hoehne M., Selbig J., Fernie A.R., Altmann T., Stitt M., 2009. Starch as a major integrator in the regulation of plant growth. Proc. Natl. Acad. Sci. USA 106 (25), 10348-10353.

Tagliani A., Tran A.N., Novi G., Di Mambro R., Pesenti M., Sacchi G.A., Perata P., Pucciariello C., 2020. The calcineurin β-like interacting protein kinase CIPK25 regulates potassium homeostasis under low oxygen in *Arabidopsis*. J. Exp. Bot. 71 (9), 2678-2689.

Tang R.-J., Wang C., Li K., Luan S., 2020. The CBL-CIPK calcium signaling network: unified paradigm from 20 years of discoveries. Trends Plant Sci. 25 (6), 604-617.

Villeret V., Huang S., Fromm H.J., Lipscomb W.N., 1995. Crystallographic evidence for the action of potassium, thallium, and lithium ions on fructose-1,6-bisphosphatase. Proc. Natl. Acad. Sci. USA 92 (19), 8916-8920.

Wang N., Hua H., Egrinya Eneji A., Li Z., Duan L., Tian X., 2012. Genotypic variations in photosynthetic and physiological adjustment to potassium deficiency in cotton (*Gossypium hirsutum*). J. Photochem. Photobiol. B 110, 1-8.

Wang Y., Wu W.-H., 2013. Potassium transport and signaling in higher plants. Annual Rev. Plant Biol. 64 (1), 451-476.

Wynn R.M., Ho R., Chuang J.L., Chuang D.T., 2001. Roles of active site and novel $K^+$ ion-binding site residues in human mitochondrial branched-chain α-ketoacid decarboxylase/dehydrogenase. J. Biol. Chem. 276 (6), 4168-4174.

Zeeman S.C., Kossmann J., Smith A.M., 2010. Starch: its metabolism, evolution, and biotechnological modification in plants. Annual Rev. Plant Biol. 61, 209-234.

Zhong W., Li K., Cai Q., Guo J., Yuan M., Wong Y.H., Walkinshaw M.D., Fothergill-Gilmore L.A., Michels P.A.M., Dedon P.C., Lescar J., 2020. Pyruvate kinase from *Plasmodium falciparum*: Structural and kinetic insights into the allosteric mechanism. Biochem. Biophys. Res. Commun. 532: 370-376.

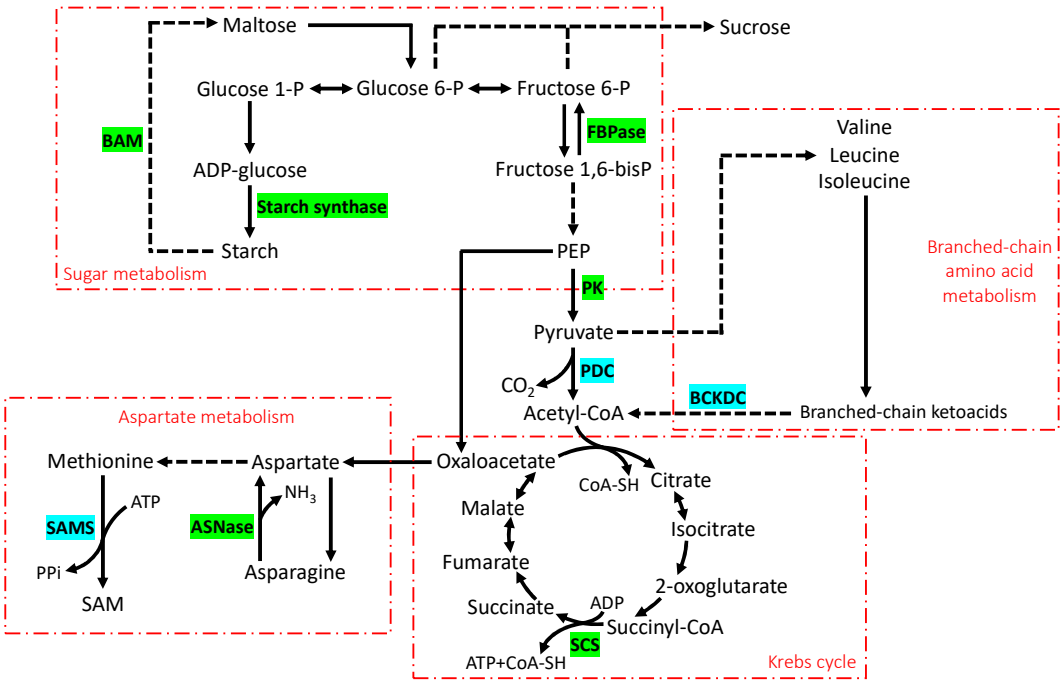


**Figure 1. Overview of $K^+$-requiring enzymes in metabolic pathways.** Plant enzymes that were shown to require $K^+$ are shown in green boxes. Enzymes in blue boxes are ubiquitously present in animals, bacteria and plants and were shown to require $K^+$ for activation in animal or bacteria but $K^+$ activation has not yet been shown experimentally in the plant enzyme. Abbreviations: ASNase, asparaginase; BAM, β-amylase; BCAT, branched-chain aminotransferase; BCKDC, branched-chain α-keto acid dehydrogenase complex; FBPase, fructose 1,6-bisphosphatase; PDC, pyruvate dehydrogenase complex; SAMS, S-adenosylmethionine synthetase (also known as methionine adenosyltransferase); SCS, succinyl-CoA thiokinase (succinyl coenzyme A synthetase).

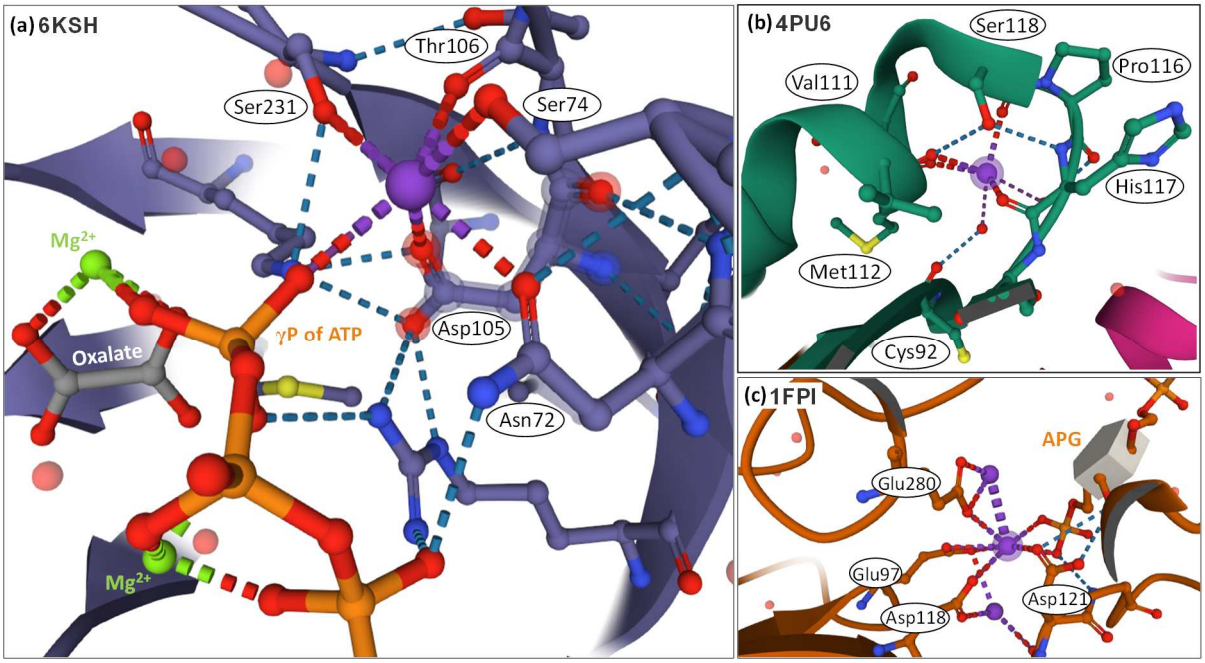


**Figure 2. Potassium binding sites in pyruvate kinase, asparaginase and fructose 1,6-bisphosphatase**. Enzyme structures shown here are (a) pyruvate kinase from *Plasmodium falciparum* (PDB number 6KSH) bound to ATP, $Mg^{2+}$, $K^+$ and oxalate, (b) asparaginase from French bean (*Phaseolus vulgaris*) bound to aspartate and $K^+$ (4PU6) and (c) fructose 1,6-bisphosphatase from pig (*Sus scrofa*) bound to AMP, 2,5-anhydro-1,6-di-O-phosphono-D-glucitol (APG; fructose 1,6-bisphosphate analogue) and $K^+$ (1FPI). Note that in the latter, the potassium binding site comprises three $K^+$ ions. Amino acid residues involved in $K^+$ binding are indicated in ellipses. This figure has been generated using structures published in (Zhong et al., 2020, Bejger et al., 2014, Villeret et al., 1995).

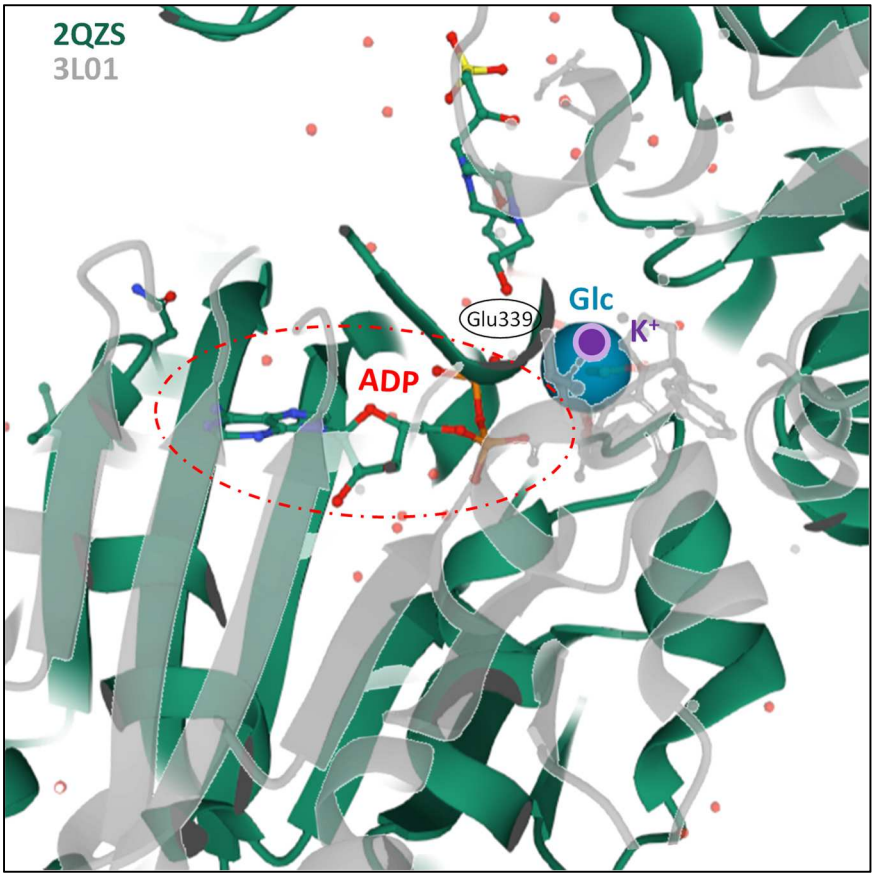


**Figure 3. Superposition of glycogen synthase structures**, from *E. coli* (PDB number 2QZS, green) with that from *Pyrococcus abyssi* (PDB number 3L01, grey). The region of ADP binding is shown with a dotted red ellipse, and glucose (Glc) position appears as a dark turquoise ball. The $K^+$ ion appears as purple disc. In the enzyme, it is probably coordinated not only to Glu 339 (which would appear just behind Glc in this representation) but also a phosphate group of ADP, which is at a short distance of a few Å. Small red balls represent solvent water. This figure has been generated using structures published in (Sheng et al., 2009, Diáz et al., 2011).

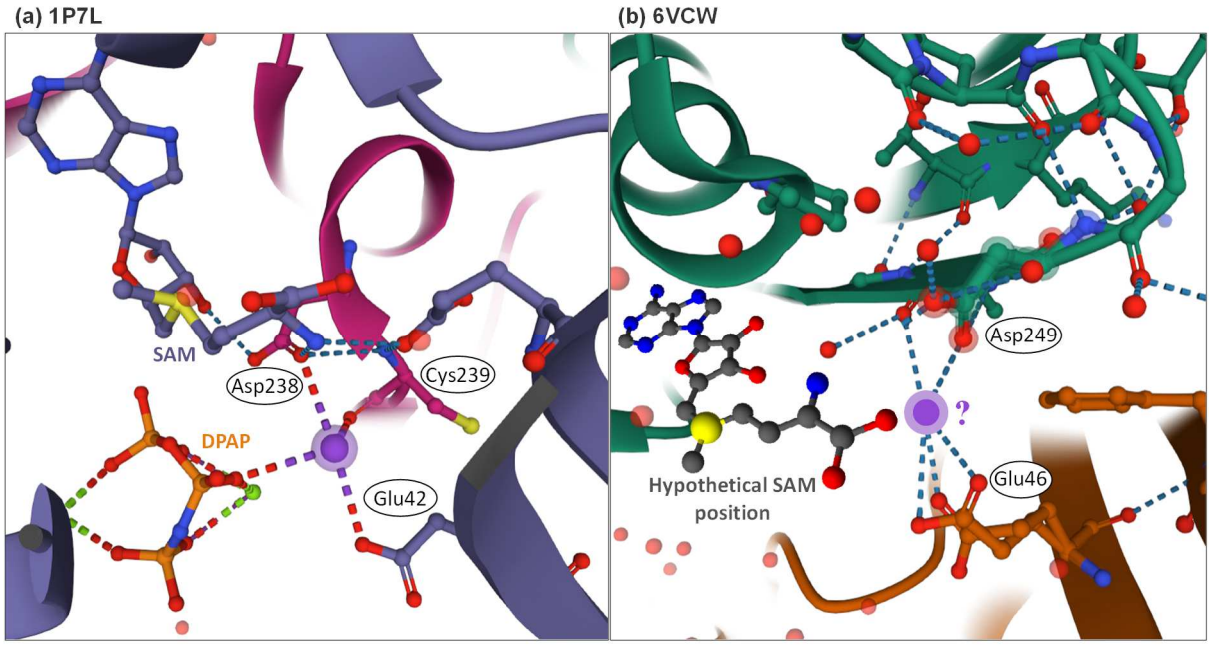


**Figure 4. Comparison of $K^+$ binding sites in SAM synthase**: structure of the bacterial (*Escherichia coli*) enzyme (a) and the plant enzyme (*Medicago truncatula*) (b). The plant enzyme (PDB number 6VCW) has been crystallized without $K^+$ and the presumed site based on homologous amino acid residues is shown (potential position of $K^+$ labelled with a question mark). SAM has been added to the structure to show its hypothetical position. Homologous aspartate and glutamate residues essential for $K^+$ binding are shown with ellipses. In both enzymes forms, the active site is situated between the extremity of a β sheet and a loop. The bacterial enzyme is bound to (diphosphono)aminophosphonic acid (DPAP), which is an analogue of the leaving phosphate groups during the reaction of SAM synthesis from ATP. This figure has been generated using structures published in (Komoto et al., 2004, Sekula et al., 2020).

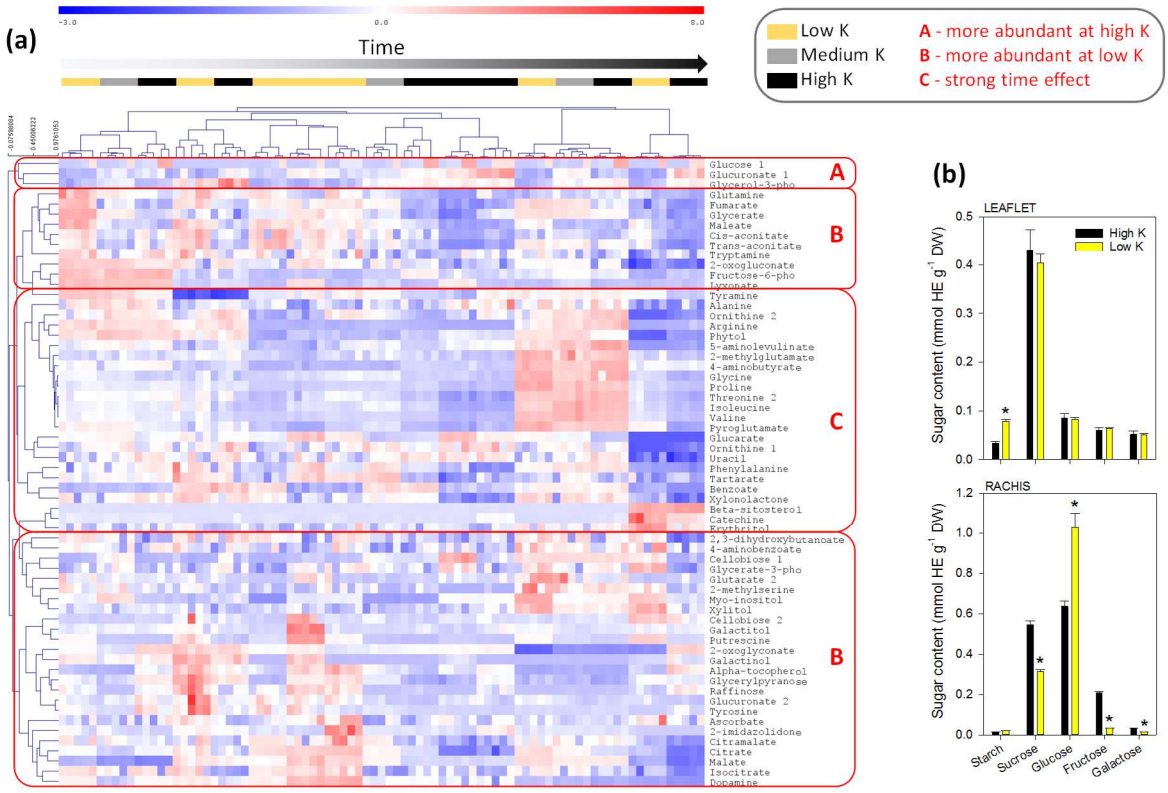


**Figure 5. Metabolic effects of K availability: example of oil palm (*Elaeis guineensis*) leaves**. Heat map showing leaflet metabolites significantly ($P$<0.01, two-way ANOVA) affected by K availability (a), and absolute content of sugars (in both leaflet and rachis) (b), in 11-month saplings. In (b) asterisks stands for statistical significance ($P$<0.01). In (a), note the important effect of sapling age on many metabolites (in particular group C where the effect of K varies with age). Groups A and B gather metabolites that are generally more (less) abundant at high (low) K availability, respectively. In (b), note the modest effect of K (only significantly more starch at low K) while the K effect on rachis concerns all soluble sugars showing the impact on sugar export from leaves. Redrawn from source data in Cui et al., 2020.

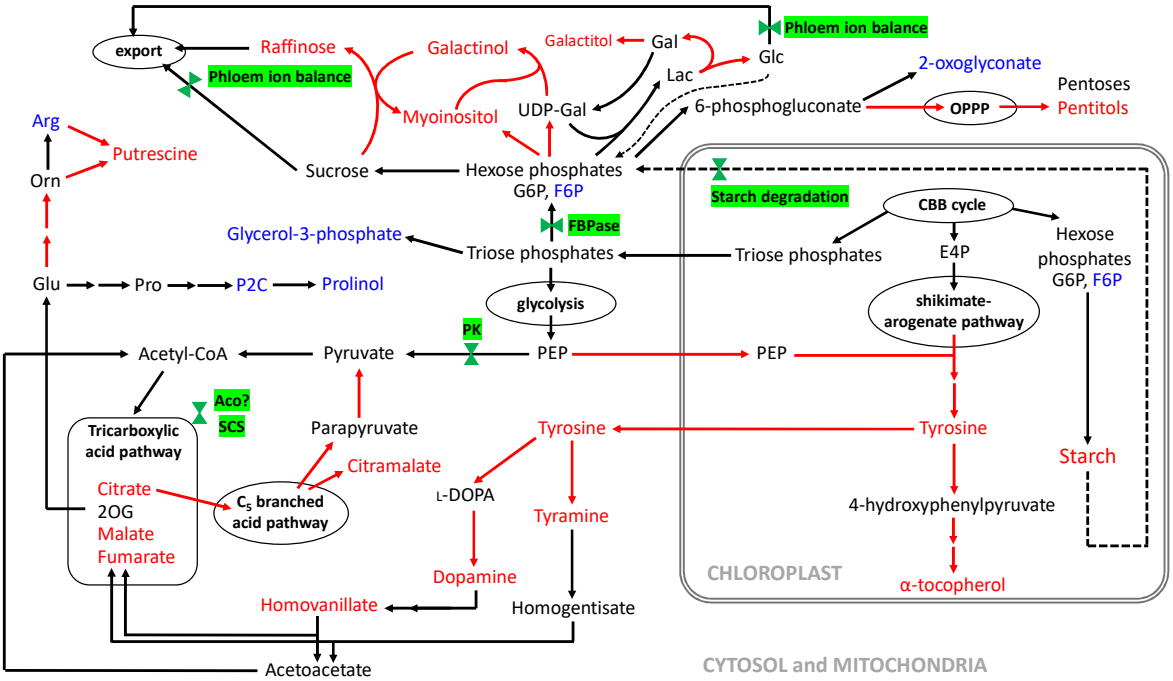


**Figure 6. Summary of low K effects on metabolic pathways**. This figure summarizes metabolic effects in oil palm, which is the best model plant documented so far by metabolomics under low K. In particular, in this species, pyruvate synthesis is achieved via parapyruvate while in *Arabidopsis*, it probably involves PEP carboxylase and malic enzyme. Key steps affected by K are shown in green. In addition to enzymes discussed in the present paper, export of sucrose and glucose, which depends on $H^+/K^+$ transport, is shown in green as being affected by low K. In red, metabolites that are more abundant at low K, in blue, metabolites less abundant at low K. The five most important effects of low K are: increase in polyamines metabolism (putrescine), alteration of sugar export and starch degradation leading to starch, raffinose and myoinositol accumulation; reconfiguration of the oxidative pentose phosphate pathway; changes in catabolism alleviating the inhibition of pyruvate kinase and Krebs cycle enzymes (aconitase, succinate thiokinase); and stimulation of tyrosine metabolism, which consumes PEP. Abbreviations: Aco, aconitase; Arg, arginine; CBB, Calvin Benson Bassham cycle; L-DOPA, L-3,4-dihydroxyphenylalanine; E4P, erythrose 4-phosphate; F6P, fructose 6-phosphate; G6P, glucose 6-phosphate; Gal, galactose; Glc, glucose; Glu, glutamate; Lac, lactose; OPPP, oxidative pentose phosphate pathway; Orn, ornithine; P2C, pyrrole-2-carboxylate; PEP, phospho*enol*pyruvate; Pi, inorganic phosphate; PK, pyruvate kinase; Pro, proline; SCS, succinate thiokinase. Pathways that are certainly up-regulated appear in red.